Soil & Tillage Research 160 (2016) 23–33

Contents lists available at ScienceDirect

Soil & Tillage Research

journal homepage: www.elsevier.com/locate/still

Carbon and nitrogen mineralization in hierarchically structured aggregates of different size

Carolin Bimüller[a,*], Olivia Kreyling[a], Angelika Kölbl[a], Margit von Lützow[a], Ingrid Kögel-Knabner[a,b]

[a] Chair of Soil Science, Research Department Ecology and Ecosystem Management, TUM School of Life Sciences Weihenstephan, Technical University of Munich, 85350 Freising-Weihenstephan, Germany
[b] Institute for Advanced Study, Technical University of Munich, Lichtenbergstraße 2a, 85748 Garching, Germany

ARTICLE INFO

Article history:
Received 24 July 2015
Received in revised form 13 December 2015
Accepted 24 December 2015
Available online xxx

Keywords:
Microbial biomass carbon and nitrogen
Grassland soil
Incubation experiment
Heterotrophic respiration
Aggregate hierarchy
Dolomite

ABSTRACT

Soil organic matter pools are turned over at different rates, but uncertainty persists regarding how far the hierarchically organized soil structure controls the mineralization dynamics. To better understand carbon and nitrogen mineralization in undisturbed aggregate classes (coarse aggregates: 2–6.3 mm, fine aggregates: <2 mm), we conducted a long-term (224-days) laboratory incubation experiment. A grassland soil (Haplic Cambisol) was chosen since its aggregates were not disturbed by tillage. The field-moist aggregate size classes were separated by a gentle dry-sieving method. We monitored the CO_2–C and NH_3–N emissions, nitrogen mineralization, pool sizes of total and salt extractable (0.5 M K_2SO_4) organic carbon and nitrogen, and microbial biomass carbon and nitrogen. By this approach, we could distinguish between the carbon and nitrogen mineralization processes of two soil aggregate size classes, relative to undisturbed bulk soil. The classes showed different aggregate architectures with variously sized subunits, but confirmed the aggregate hierarchy. For both aggregate classes, the recombined sum of respired CO_2–C per unit of soil organic carbon equaled the bulk soil, proving that our aggregate separation preserved the original aggregates as intact functional units. Both aggregate size classes and the bulk soil respired only 4% soil organic carbon throughout the incubation period. The coarse aggregates, which mostly comprised small macroaggregates, mineralized more carbon per unit soil organic carbon than the fine aggregates (composed of microaggregates), indicating a higher bioavailability of soil organic matter in the coarse aggregates. Accordingly microbial metabolic efficiency was higher in coarse than in fine aggregates. Nitrogen mineralization was higher in fine aggregates than in coarse aggregates, but was impaired by carbon limitation as the incubation experiment proceeded. We conclude that bioavailability of soil organic matter was affected by different aggregate architectures in the different aggregate size classes. The lower bioavailability of soil organic matter in fine aggregates is due to an enhanced stabilization through cation bridging of the dolomitic soil material at the microaggregate level, whereas the higher soil organic matter bioavailability in coarse aggregates is explained by labile organic components at the macroaggregate level.

1. Introduction

Soil aggregation depends on the soil fauna, microorganisms, roots, organic and inorganic binding agents, and environmental and physical forces (Oades, 1993; Six et al., 2004). Neutral to alkaline soils with C/N ratios <15, derived from calcareous parent material with mull humus form, are characterized by low proportions of organic matter present as plant debris (Oades, 1984, 1988). Under these slightly alkaline conditions, calcium and magnesium cations preferentially form bridges between negatively charged clay colloids and negatively charged soil organic matter (SOM), enhancing the stability of the aggregate system (Baldock et al., 1997; Baldock and Skjemstad, 2000; Bockenhoff et al., 1997; Oades, 1988; Rashad et al., 2010). These polyvalent metal ions ensure the integrity of microaggregates and other persistent organic materials (Elliott, 1986; Tisdall and Oades, 1982).

Previous studies on aggregate carbon mineralization have focused on land use (Akinsete and Nortcliff, 2014; Gupta and Germida, 1988; Rabbi et al., 2015) and tillage systems (Beare et al., 1994; Fernandez et al., 2010; Nyamadzawo et al., 2009; Six et al.,

* Corresponding author.
E-mail address: carolin.bimueller@wzw.tum.de (C. Bimüller).

http://dx.doi.org/10.1016/j.still.2015.12.011
0167-1987/

2000). Carbon mineralization has been altered by management practices. In a 100-day incubation study, the carbon mineralization per unit of soil organic carbon (SOC) in pastures (0.005%) was double that of arable cropping systems (0.002%) (Curtin et al., 2014). This difference is attributed to a continuous supply of labile carbon in the form of coarse organic matter from perennial vegetation, which is greatly reduced under arable cropping (Baker et al., 2007; Curtin et al., 2014). However, the stability of SOC with undisturbed natural aggregates has been little investigated (Álvarez et al., 2007). The simultaneous evaluation of carbon and nitrogen mineralization behavior in aggregates has been undertaken only recently (Curtin et al., 2014; Oorts et al., 2006), and reports of SOC and nitrogen in undisturbed aggregates remain rare. The carbon and nitrogen mineralization of aggregates is commonly evaluated in complementary laboratory studies, wherein the soils are segregated into aggregate size classes and incubated (Six and Paustian, 2014). In the laboratory experiment of Curtin et al. (2014), carbon and nitrogen mineralization was calculated by the increased surface area with decreasing aggregate size.

Nevertheless, despite some studies (Gupta and Germida, 1988; Sainju et al., 2009; Zhang et al., 2012) researching the distribution of microbial biomass carbon (MBC) and nitrogen (MBN) in different aggregate classes, and how this biomass relates to SOM mineralization in each aggregate class, this topic still remains poorly understood. Miller and Dick (1995) found a qualitative difference in the microbial communities occupying macro- and microaggregates. Gupta and Germida (1988, 2015),) emphasized the importance of microbial biomass in the formation of macroaggregates and as a primary source of SOM for carbon mineralization. They identified a crushing effect of the macroaggregates, which enhances carbon mineralization. This disruption releases the microbial biomass mucilage that binds the macroaggregates, which contributes to the mineralizing SOM. Therefore, by collecting data on MBC and MBN and the community structure across aggregate size classes, we can begin to elucidate carbon and nitrogen cycling (Six and Paustian, 2014) and their coupling as determined by the soil structure.

To better understand the coupled regulation of carbon and nitrogen mineralization in undisturbed aggregates, we conducted an incubation experiment. We studied mineralization in two aggregate size classes of a dolomitic grassland soil (Haplic Cambisol), composed of different hierarchically organized substructures. Specifically, we asked the following questions: (1) Do different aggregate classes mineralize at similar rates when their water and air availabilities are comparable? (2) Do aggregate size classes differ in their substructures, external surface areas, and bioavailability of SOM? (3) Do aggregate classes of different sizes exhibit diverse heterotrophic respiration efficiencies? Thus, the present study seeks to identify the role of different intact structural units to the overall soil mineralization of carbon and nitrogen as controlled by bioavailability in aggregate substructures.

2. Materials and methods

2.1. Site characteristics and origin of soil material

The sampling site Graswang is located near Garmisch–Partenkirchen in a foothill valley (877 m above sea level) of the German limestone Alps in southern Bavaria. This area is designated as permanent grassland (Unteregelsbacher et al., 2013). Soil material for the incubation study was collected from the Ah horizon (10–15 cm) of a Haplic Cambisol (Calcaric, Humic, Siltic) (IUSS Working Group WRB, 2014) underneath the main rooting zone in the fall of 2009. The parent material is dolomitic alluvial gravel; the climate is characterized by a mean annual air temperature of 6.7 °C and a precipitation of 1757 mm (Kreyling et al., 2013). Undisturbed soil samples were taken under field-moist conditions. To preserve their microbial communities, the samples were stored under cooled conditions (4 °C) prior to further preparation (Petersen and Klug, 1994). Material was well-aggregated by the abiotic dolomitic parent material and free particulate organic material was almost absent (Kreyling et al., 2013). The texture was dominated by silt (68%), with minor quantities of clay (22%) and sand (10%) (Unteregelsbacher et al., 2013). The pH was 7.1 and the organic carbon and total nitrogen concentrations were 57 ± 4 and $6.1 \pm 2.0\,mg\,g^{-1}$, respectively, corresponding to a C/N ratio of 9.

2.2. Soil preparation and incubation

We separated and incubated three aggregate size classes of the sampled soil material from the Ah horizon. The material in the bulk soil class was not processed, since we wanted to conserve the intact aggregation. For both aggregate classes, the complete field-moist soil samples were gently separated into macroaggregates <6.3 mm using a sieve (Kölbl et al., 2005). Fragments such as roots and stones constituted a negligible share and were removed. The resulting aggregates were subdivided into coarse (2–6.3 mm) and fine aggregates (<2 mm) by sieving

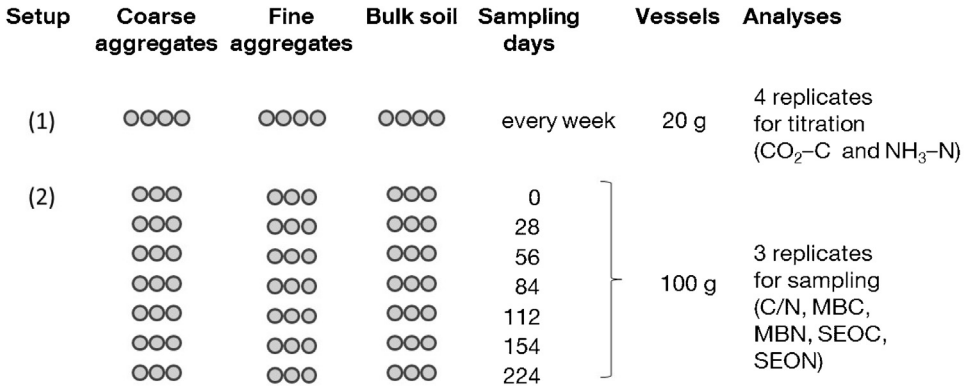

Fig. 1. Experimental setups: (1) for titration and (2) for sampling. MBC: microbial biomass carbon; MBN: microbial biomass nitrogen; SEOC: salt extractable organic carbon; and SEON: salt extractable organic nitrogen.

through a 2-mm sieve. This cut-off was selected as the most feasible cut-off for aggregate fractionation in a series of preliminary experiments, conserving larger entities visible from the natural soil. The coarse and fine aggregates comprised 79 mass% and 21 mass% of the bulk soil, respectively. We calculated a mathematical recombination of both aggregate size classes for all measured parameters using these mass proportions and named it recombined bulk soil.

We incubated bulk soil, coarse aggregates, and fine aggregates in two experimental setups. In the first setup, CO_2 and NH_3 productions were measured (four replicates per sample) weekly throughout the 32-week incubation period. In the second setup, an additional three replicates were destructively sampled at five time points for analysis of MBC and MBN, and at seven time points for nitrogen mineralization analysis (Fig. 1). In both incubation settings, coarse aggregates, fine aggregates, and bulk soil were weighed in vessels prepared from plastic pipes. The walls of each vessel were perforated to ensure sufficient air exchange (Mueller et al., 2012), and their bases were prepared from a glass fiber filter (Bimüller et al., 2014). Soil loss was prevented by inserting fine meshed nylon fabric along the vessel interiors. The CO_2–C and NH_3–N emissions were monitored in small vessels (inner diameter: 36 mm, height: 50 mm) filled with 20 g soil ($vessel_{20g;}$ setup 1); nitrogen mineralization and MBC and MBN were measured in larger vessels (inner diameter: 70 mm, height: 60 mm) filled with 100 g soil ($vessel_{100g;}$ setup 2). By designing two vessel sizes, we guaranteed similar air-exchangeable soil surfaces per soil volumes. The bulk densities in all incubated samples ranged from 0.8 to 1.0 g cm^{-3}, which are realistic for an intensively rooted grassland topsoil similar to the values found at the field site Graswang. Prior to incubation, all vessel samples were water saturated with distilled water and were allowed to equilibrate for 24 h. Vessels were subsequently placed on suction plates in the dark under a vacuum pressure of 300 hPa (pF 2.5) for 14 days. This pre-incubation did not change volume and bulk density, but removed the first flush of carbon respiration triggered by rewetting (Franzluebbers et al., 1996). The experimental approach ensured appropriate hydrological conditions, with water saturated meso- and micropores <10 μm across, and sufficient oxygen provided by dewatering of macropores >10 μm. Subsequently, the coarse aggregates, fine aggregates, and bulk soil were incubated in 1 l airproof jars for 32 weeks (224 days) in the dark at 20 °C. Water contents were controlled by weighing the soil samples at eight week intervals during the incubation. If the water loss exceeded 2%, the deficit was replaced by a calibrated spray flask. All jars were weekly opened to allow air exchange. By this approach, we strove for comparable initial conditions of all samples.

2.3. Measurement of CO_2 and NH_3 emissions (setup 1)

Incubation jars for CO_2–C and NH_3–N measurements were equipped with two tins, containing 10 ml 0.1 M NaOH and 10 ml 2% H_3BO_3 to trap the emitted CO_2 (Alef and Nannipieri, 1995) and NH_3, respectively (displayed in graphical abstract). Both aggregate size classes and the bulk soil were incubated in quadruplicate and their gas emissions were determined weekly, yielding 32 times measurements (setup 1). Four control jars containing pure NaOH and H_3BO_3 were also prepared. Carbon mineralization was calculated as the difference in CO_2 adsorption between the treatments (aggregate size classes or bulk soil) and the control. The inorganic carbon (IC) concentrations were monitored over the experimental period by combustion in a muffle furnace (Kreyling et al., 2013) and were found to be constant. We therefore assume that carbon mineralization originated only from organic carbon respiration (Bertrand et al., 2007).

2.4. Determination of nitrogen mineralization and microbial biomass carbon and nitrogen (setup 2)

Soil moisture contents, MBC and MBN, NH_4^+–N, NO_3^-–N, and total SOC and nitrogen (N_{tot}) were measured in triplicate for each sample. Nitrogen mineralization was measured on days 0, 28, 56, 84, 112, 154, and 224 of the incubation. Microbial biomass was determined on five dates (day 0, 14, 28, 84, and 224).

For NH_4^+–N and NO_3^-–N determination, 10 g subsampled soil were shaken in 100 ml 2 M KCl for 1 h. Extracts were filtered through cellulose filters (2 V, Whatman, Maidstone, England) and photometrically measured (Spectronic 601, Milton Roy, Rochester NY, USA). Following Schlichting et al. (1995), the extracts in the NH_4^+–N determination were reacted with salicylate-citrate and reagent solutions and were measured at 655 nm. The extracts in the NO_3^-–N determination were reacted with salicylic acid and sodium hydroxide and were measured at 410 nm.

Microbial biomass was determined by fumigation–extraction (Vance et al., 1987). Briefly, a 25-g aliquot of soil was fumigated with ethanol-free $CHCl_3$ for 24 h. Subsequently, the soil was extracted with 100 ml 0.5 M K_2SO_4 for 30 min in a horizontal shaker. A second 25-g aliquot was extracted without previous fumigation. To ensure that chloroform homogeneously accessed the soil surfaces, we crushed and sieved the bulk soil and the coarse aggregates to <2 mm. Subsequently, the fumigated and non-fumigated samples were filtered through a 0.45 μm cellulose nitrate filter (Sartorius Stedim, Göttingen, Germany). After the addition of two drops HCl, the total organic carbon (TOC) and total bound nitrogen (TNb) of the extracts were measured using a DIMA-TOC 2000 instrument (Dimatec, Essen, Germany). For calculating the MBC and MBN concentrations, the TOC values were divided by 0.45 and TNb values by 0.54, respectively (Vance et al., 1987). Metabolic quotients were calculated from the respired CO_2–C and expressed in milligrams per unit MBC. The control values of the corresponding non-fumigated samples were assumed to approximate the salt-extractable organic carbon (SEOC) and salt-extractable organic nitrogen (SEON), respectively.

2.5. Soil moisture and carbon and nitrogen contents (setup 2)

At each of the seven $vessel_{100g}$ sampling dates (setup 2), a 15-g aliquot of moist soil was taken, dried at 105 °C for 24 h, and reweighed to determine its soil moisture content. The means of three replicates were calculated. Subsequently, the dried soil material was finely ground (Pulverisette 23, Fritsch, Idar-Oberstein, Germany) and its carbon and nitrogen concentrations were measured before and after treatment in a muffle furnace at 450 °C for 4.5 h, which combusted any organic matter. Duplicate samples of three replicates were analyzed for total carbon and nitrogen by dry combustion at 1000 °C (EuroEA 3000, Hekatech, Wegberg, Germany). The carbon in heat-treated samples was considered exclusively as IC; the carbon in the untreated samples represented the total C. SOC concentrations were calculated by subtracting IC from the total C.

2.6. Analysis of aggregate substructures

To characterize the substructure of the macroaggregate size classes, we ultrasonically dispersed 30 g of coarse and fine aggregates (Sonoplus HD2200, Bandelin, Berlin, Germany) using an energy input of 60 J ml^{-1} as described in Amelung and Zech (1999). The ultrasonication breaks up the larger macroaggregates without destroying sensitive soil constituents such as particulate organic materials. Subsequently, the soil was wet-sieved into five substructural aggregate size classes: >630 μm, 200–630 μm,

63–200 μm, 20–63 μm, and <20 μm. These aggregate size classes were freeze-dried and weighed.

2.7. Statistical analysis

For a detailed comparison of the mineralization processes, we fitted the measured values to two pool first-order exponential models ($R^2 > 0.98$) (Bimüller et al., 2014; Collins et al., 2000; Stemmer et al., 1999) using SigmaPlot 11.0 (Systat Software Inc., San José (CA), USA):

$$C(t) = C_r \exp(-k_r \times t) + C_s \exp(-k_s \times t) \quad (1)$$

$C(t)$ is the amount of respired carbon at time t. $C(t)$ embodies the mineralization from two pools with different decomposability, a relatively fast mineralizable pool modeled with constant C_r and a more slowly mineralizable carbon pool with constant C_s. k_r and k_s are the corresponding rate coefficients, and t is the incubation time. All statistical analyses were conducted with SPSS 22 (IBM SPSS Statistics, Ehningen, Germany). Significant differences in cumulative carbon mineralization were tested at 7 and 224 days for each fraction. Nitrogen mineralization was checked at all sampling dates, differentiating among the fractions. All t-tests were conducted at the $\alpha = 0.05$ significance level. Prior to the t-tests, specific data sets were tested for normal distribution using the Shapiro–Wilk test and checked for variance homogeneity using Levene's test.

3. Results

3.1. Characterization of incubated aggregate size classes

The coarse and fine aggregate size classes showed distinctly different substructures of micro- and macroaggregates (Fig. 2). The coarse aggregates comprised macroaggregates >630 μm (43%), whereas fine aggregates comprised mainly microaggregates <20 μm (53%). On the contrary, 90% of the fine aggregates were microaggregates <63 μm, whereas microaggregates <63 μm comprised only 40% of the coarse aggregates.

After (pore-size dependent) dewatering on suction plates to field capacity (pF 2.5) prior to incubation, the water contents of the samples were similar, ranging from 46 to 49 mass% (average: 48 mass%) (Table 1). The dolomite (7%–8%), organic carbon contents (6%–7%) and other minerals built up to an average specific density of 2.6 g m^{-3}. Given that the average bulk density was 0.9 g cm^{-3}, the calculated total pore volume was 65 vol%. The average volumetric water content at pF 2.5 was 43 vol%. Thus, air constituted 22 vol%, indicating well-aerated soil conditions. These conditions resemble natural conditions under field capacity.

Initial SOC and N_{tot} concentrations increased from bulk soil over coarse aggregates to fine aggregates (Table 1), and remained largely constant throughout the incubation time. The OC/N ratios of the coarse aggregates, fine aggregates and bulk soil were the same (9 ± 1). The IC values were constant throughout the incubation (7%–8% in all classes), since dolomite is hardly soluble. We therefore considered CO_2 evolution rates to solely represent respired carbon from SOC mineralization.

3.2. Carbon mineralization

The carbon mineralization rates in both aggregate size classes and bulk soil declined over the 224 days' incubation (Fig. 3). Eq. (1) assumes that carbon is available in two pools; one rapidly mineralizable the other slowly mineralizable. The mineralization rates of these carbon pools are described by separate terms in Eq. (1) (Fig. 3). The theoretical tipping point of the individual pools is the time at which both pools equally contribute to the mineralized carbon. In both aggregate classes and the bulk soil, the tipping point occurred at approximately 11 days. Thereafter, most of the respired carbon originated from the slower pool.

According to the cumulative carbon mineralization rates, the fine aggregates emitted more CO_2–C per mass soil and less CO_2–C per unit mass SOC than the other size classes (Fig. 4). The cumulative CO_2–C mineralization per unit mass SOC significantly differed between the fine aggregates and the other size classes after 224 days, but had already begun deviating at 7 days. After 224 days, all size classes had mineralized only around 4% of their SOC.

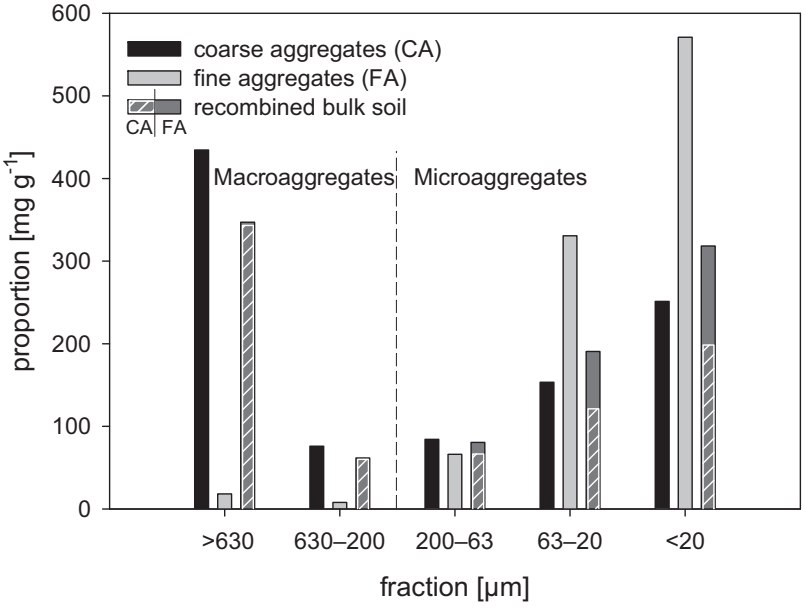

Fig. 2. Substructures of aggregate classes consisting of smaller macro- and microaggregates: Five fractions were obtained by ultrasound (60 J ml^{-1}) and wet sieving. The hatched sections of the recombined bulk soil bars indicate the proportion of coarse aggregates in the recombined bulk soil.

Table 1
Concentrations of total carbon, inorganic carbon (IC), soil organic carbon (SOC) and total nitrogen (N_{tot}), OC/N ratios, and water contents of coarse aggregates, fine aggregates, and bulk soil. Results are the mean values and standard deviations of three replicates at the beginning of incubation.

	Total C (mg g^{-1})	IC (mg g^{-1})	SOC (mg g^{-1})	N_{tot} (mg g^{-1})	SOC/N	Water content (mass%)
Coarse aggregates	138 ± 1	76 ± 1	62 ± 0	7.0 ± 0.8	9 ± 1	48 ± 3
Fine aggregates	143 ± 5	74 ± 1	70 ± 6	7.1 ± 0.1	10 ± 1	49 ± 1
Bulk soil	134 ± 2	77 ± 2	57 ± 4	6.1 ± 2.0	9 ± 0	46 ± 2

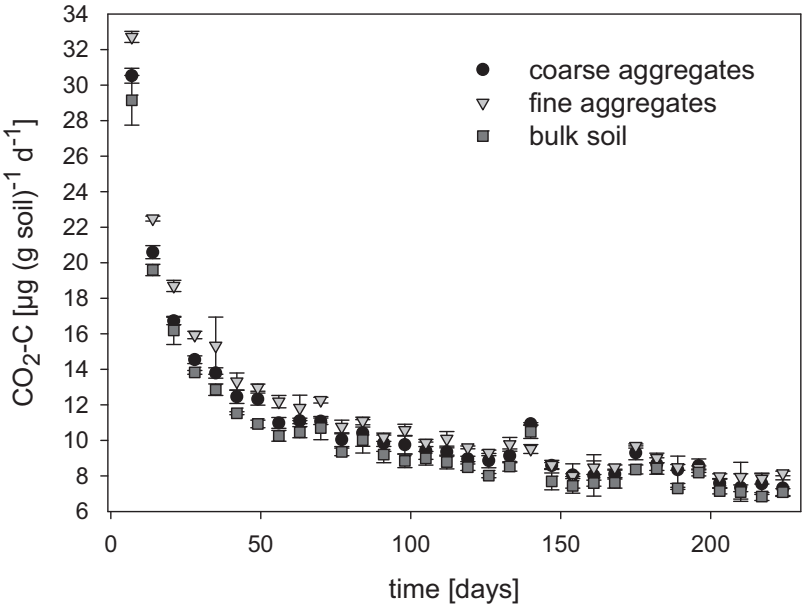

Fig. 3. CO_2–C respiration rates (µg per g soil per day) in coarse aggregates, fine aggregates, and bulk soil. Means ($n = 4$) and standard deviations are shown. The measured values were fitted to the two-component exponential decay model, yielding the following equations:
coarse aggregates: $y = 34.5 \times e^{-0.0960 \cdot t} + 12.8 \times e^{-0.0025 \cdot t}$ $R^2 = 0.98$
fine aggregates: $y = 34.3 \times e^{-0.0861 \cdot t} + 13.8 \times e^{-0.0027 \cdot t}$ $R^2 = 0.98$
bulk soil: $y = 32.8 \times e^{-0.0921 \cdot t} + 11.8 \times e^{-0.0024 \cdot t}$ $R^2 = 0.98$.

3.3. Nitrogen mineralization

The NH_3 emissions remained below the detection limit throughout the incubation time (data not shown). At 0 days, NH_4^+–N comprised 61%–72% of the total N_{min} concentration (Fig. 5a and b). Thereafter, the NH_4^+–N concentrations rapidly decreased, falling to 10%–22% of the total N_{min} and did not show any trend thereafter (Fig. 5b). The total N_{min} concentration, calculated by summing the NH_4^+–N and NO_3–N concentrations, showed no clear trend over the incubation time (Fig. 5). Among all size classes, the mean concentrations of mineralized nitrogen varied between 6.0 and 9.6 mg $(g\,N_{tot})^{-1}$, with the higher concentrations found in the fine aggregates. After 224 days, the mineralized nitrogen decreased to its minimum in every sample. The N_{min} significantly differed between the fine aggregates and all other fractions (Fig. 5a and b). The N_{min} per unit mass soil also significantly differed between the bulk soil and coarse aggregates, and between the bulk and recombined bulk soil (Fig. 5a).

3.4. Microbial biomass carbon and nitrogen development

Overall, MBC and MBN decreased with incubation time (Table 2). The trend was most obvious in the fine aggregates, whose initial MBC and MBN concentrations were the highest among the size classes (24 mg $(g\,SOC)^{-1}$ and 37 mg $(g\,N_{tot})^{-1}$, respectively) and smallest at the end of the experiment (12 mg $(g\,SOC)^{-1}$ and 4 mg $(g\,N_{tot})^{-1}$, respectively). After 224 days, the MBC of fine and coarse aggregates had decreased to 50% and 75% of their initial values, respectively. Meanwhile, the MBN values of fine and coarse aggregates had declined to 11% and 34%, respectively, of their initial values. On the penultimate and final sampling dates, the MBC and MBN levels approached the detection limit, thereby showing large standard deviations. While the MBC and SEOC both declined over time, the decrease in MBN was accompanied by an increase in SEON (Tables 2 and 3).

Bulk soil initially showed the highest metabolic quotient (0 and 14 days in Table 4), but was superseded by the fine aggregates after 28 days. At this time, the metabolic quotient of fine aggregates exceeded that of bulk soil and coarse aggregates. Furthermore, apart from small fluctuations on day 84, the metabolic quotient declined throughout the experiment in all three of the incubated size classes. The strongest decline occurred between 14 and 28 days. On day 224, the metabolic quotient was halved in nearly all size classes.

3.5. Relationship between carbon and nitrogen dynamics

The cumulative carbon was negatively correlated with nitrogen mineralization in all size classes (Fig. 6). However, the correlations were weak, ranging from $R^2 = 0.10$ (fine aggregates) to 0.28 (bulk soil). This indicates that CO_2–C evolution impeded the nitrogen mineralization. Fine aggregates presented the highest N_{min}

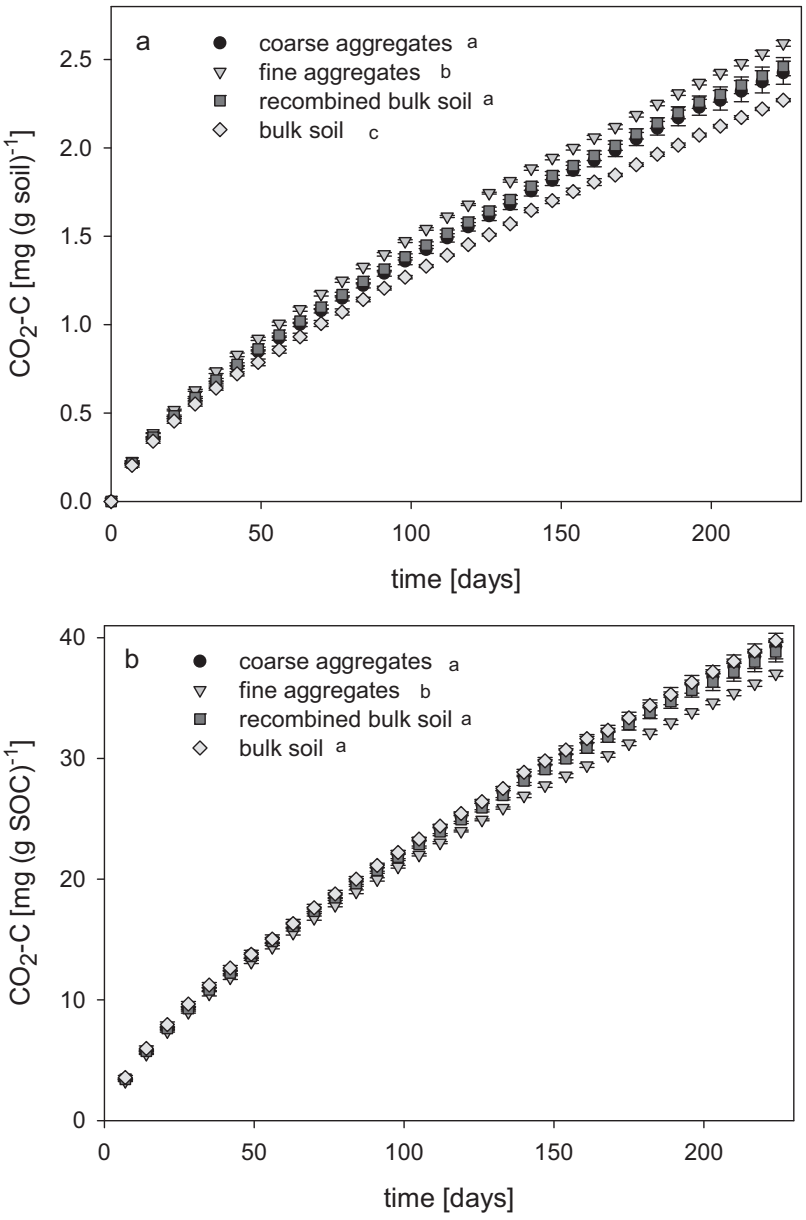

Fig. 4. (a) Cumulative CO_2–C respiration rates (mg per g soil) in coarse aggregates, fine aggregates, and bulk soil. (b) Cumulative CO_2–C concentrations in mg per g soil organic carbon (SOC) of three incubated size classes present at the beginning of the incubation. Means ($n = 4$) and standard deviations are shown. The lowercase letters indicate significant differences between the substrates measured at 224 days ($\alpha = 0.05$).

concentration per mineralized carbon. While the correlation slopes of coarse aggregates, fine aggregates and recombined bulk soil were almost identical; the decrease in N_{min} per respired CO_2–C was lower in bulk soil than in the other size classes.

4. Discussion

4.1. Architecture of macroaggregates

Both coarse and fine aggregates were hierarchically structured; that is, the smaller subunits (the microaggregates) were accumulated into larger macroaggregates. In coarse aggregates, these macroaggregates (200 μm–6.3 mm) were not disrupted by ultrasonication at 60 J ml^{-1}, indicating that the macroaggregate structures were stabilized therein. By contrast, fine aggregates exposed to this energy were almost entirely broken down into microaggregates (Fig. 2). Some of the microaggregates were naturally free in intact bulk soil, others were bound into macroaggregates. The results of this successive fractionation confirm the hierarchy concept proposed by Tisdall and Oades (1982) in our highly aggregated grassland soil. The mathematical recombination showed that coarse aggregates were predominately present in the bulk soil. Despite large architectural differences between the coarse and fine aggregates (Fig. 2), both total pore volume and water content at field capacity were similar in the incubation vessels of both aggregate size classes. Such similarity in the air and water balance has ecological implications and is related to the texture and bulk density, which are identical for all aggregates. The C/N ratios were similar in bulk soil, coarse aggregates, and fine aggregates (Table 1). Fine aggregates contained more total carbon and SOC than coarse aggregates and bulk soil, consistent with the results of Mikha and Rice (2004) and Akinsete and Nortcliff (2014), who reported the highest carbon concentrations in aggregate size classes of 250 μm–2 mm

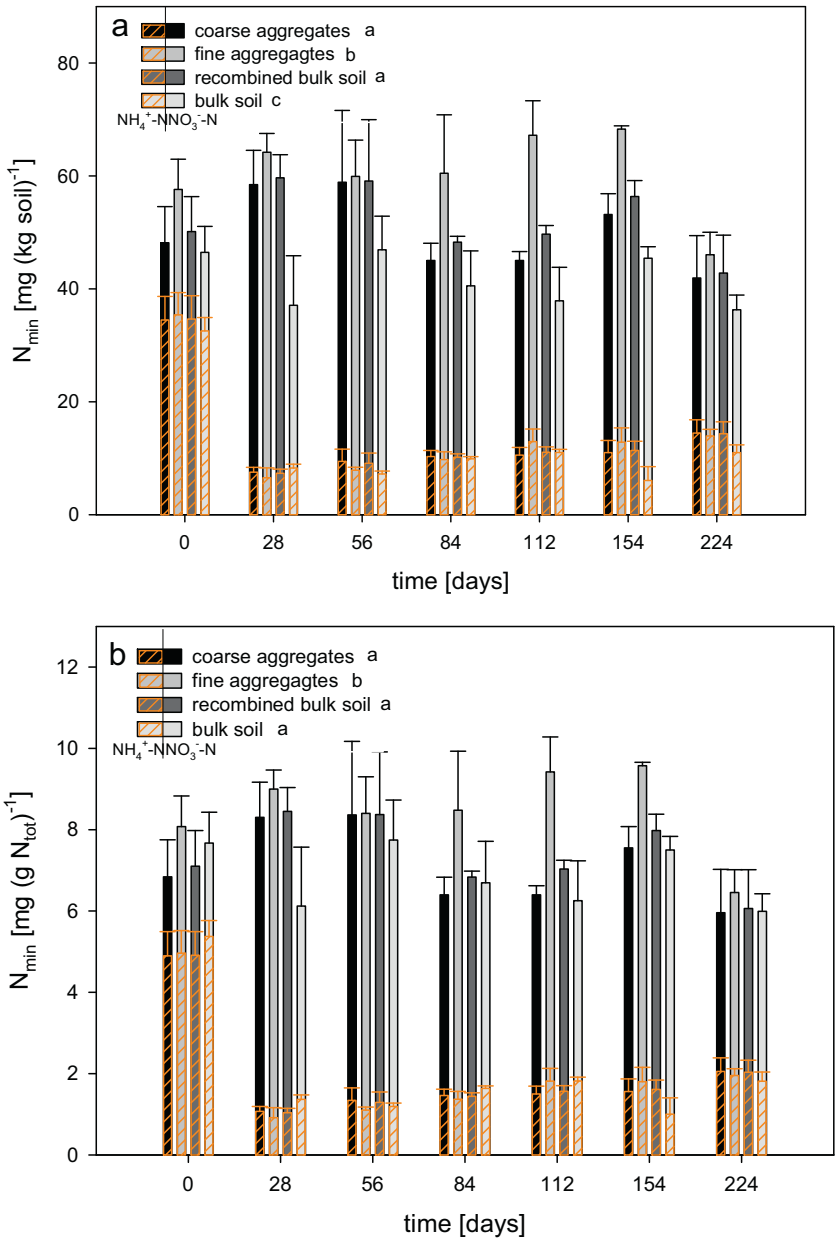

Fig. 5. Chronological sequence of mineralized nitrogen (N_{min}) concentrations (sum of NH_4^+–N and NO_3^-–N) in coarse aggregates, fine aggregates, recombined bulk soil, and intact bulk soil. N_{min} concentrations are presented as stacked column bars with hatched bars indicating the portion of NH_4^+–N in each sample. Results are expressed in (a) mg per g soil and (b) mg per g total nitrogen. Means ($n = 3$) and standard deviations are shown. Significant differences between both aggregate classes, the recombined bulk soil, and the bulk soil over all sampling days are indicated by different lowercase letters (significance level of $\alpha = 0.05$).

Table 2
Concentrations of microbial biomass carbon (MBC) and microbial biomass nitrogen (MBN) of coarse aggregates, fine aggregates, the mathematically recombined bulk soil, and intact bulk soil (means ($n = 3$) ± standard deviations).

Time (d)	MBC (mg (g SOC)$^{-1}$)				MBN (mg (g N_{tot})$^{-1}$)			
	Coarse aggregates	Fine aggregates	Recombined bulk soil	Bulk soil	Coarse aggregates	Fine aggregates	Recombined bulk soil	Bulk soil
0	24 ± 3	24 ± 1	26 ± 2	22 ± 3	38 ± 6	37 ± 3	37 ± 4	34 ± 6
14	22 ± 2	19 ± 3	23 ± 2	20 ± 4	21 ± 5	13 ± 12	20 ± 4	15 ± 9
28	24 ± 2	20 ± 0	25 ± 1	23 ± 3	23 ± 9	15 ± 5	21 ± 8	35 ± 6
84	15 ± 1	13 ± 1	12 ± 7	16 ± 1	n.d.a.	n.d.a.	n.d.a.	n.d.a.
224	18 ± 2	12 ± 1	18 ± 2	15 ± 1	13 ± 10	4 ± 2	11 ± 8	12 ± 7

n.d.a.—no data available.

Table 3
Concentrations of salt-extractable organic carbon (SEOC) and salt-extractable organic nitrogen (SEON) of coarse aggregates, fine aggregates, the mathematically recombined bulk soil, and intact bulk soil (means ($n = 3$) ± standard deviations).

Time (d)	SEOC (mg (g SOC)$^{-1}$)				SEON (mg (g N_{tot})$^{-1}$)			
	Coarse aggregates	Fine aggregates	Recombined bulk soil	Bulk soil	Coarse aggregates	Fine aggregates	Recombined bulk soil	Bulk soil
0	3.5 ± 0.4	2.4 ± 0.2	3.2 ± 0.3	3.4 ± 0.1	23.2 ± 1.5	24.2 ± 1.0	23.4 ± 1.2	25.7 ± 1.2
14	2.1 ± 0.1	2.0 ± 0.8	2.9 ± 0.1	2.9 ± 0.3	36.4 ± 0.2	49.1 ± 13.2	39.1 ± 2.8	39.7 ± 2.3
28	2.0 ± 0.3	2.2 ± 0.2	2.6 ± 0.3	2.7 ± 0.5	41.2 ± 2.8	42.7 ± 3.3	41.5 ± 2.9	36.7 ± 2.1
84	2.5 ± 1.1	2.1 ± 0.1	2.1 ± 0.8	2.5 ± 0.1	55.5 ± 23.4	48.6 ± 5.3	54.1 ± 19.6	50.2 ± 2.3
224	2.3 ± 0.2	2.2 ± 0.1	2.2 ± 0.2	2.3 ± 0.1	54.6 ± 3.4	56.6 ± 1.9	55.0 ± 3.0	57.1 ± 2.8

Table 4
Chronological sequence of metabolic quotient: concentrations of CO_2–C per mass microbial biomass carbon (MBC) per hour in coarse aggregates, fine aggregates, the mathematically recombined bulk soil, and intact bulk soil (means ($n = 12$) ± standard deviations).

Time (d)	CO_2–C (mg (g MBC)$^{-1}$ h^{-1})			
	Coarse aggregates	Fine aggregates	Recombined bulk soil	Bulk soil
14	622 ± 52	713 ± 92	641 ± 42	740 ± 130
28	406 ± 23	474 ± 9	420 ± 19	436 ± 51
84	471 ± 47	500 ± 20	480 ± 35	450 ± 36
224	279 ± 31	410 ± 23	307 ± 24	330 ± 26

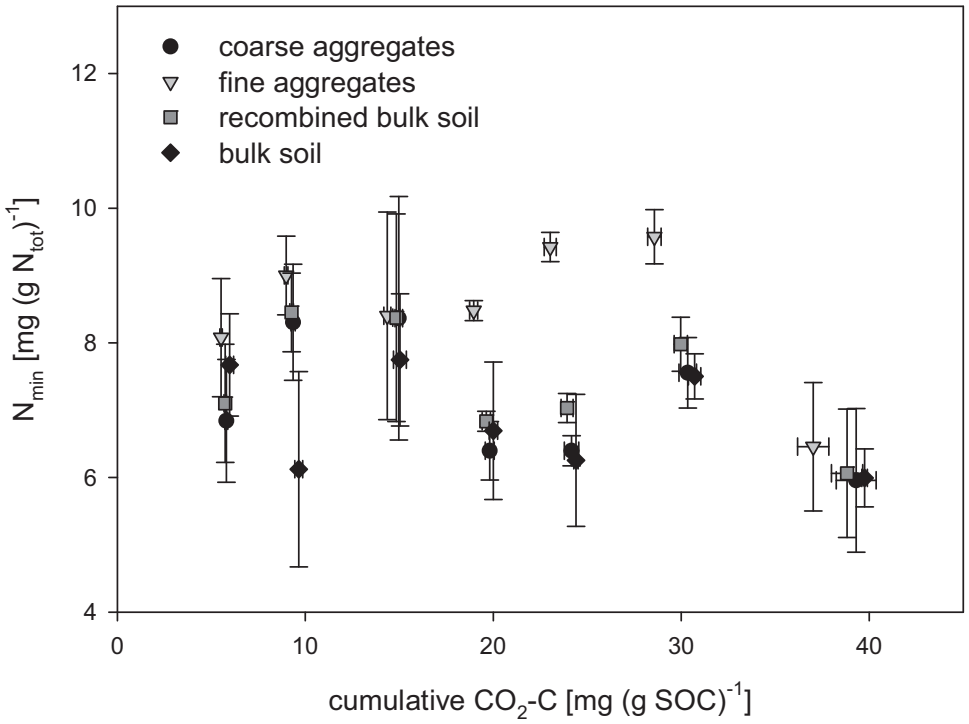

Fig. 6. Amount of mineralized nitrogen (per unit initial N_{tot}) regressed against the cumulative mineralized carbon (per unit initial SOC). CO_2–C and N_{min} values are the means and standard deviations of 4 and 3 samples, respectively.

and 1–2 mm diameter, respectively. The size classes of both groups correspond to our fine aggregate size class.

By considering the internal subunits of both aggregate classes, we can apply the aggregate hierarchy concept to the fine and coarse aggregates of our study. Both aggregate classes were composed differently according to their size, but consisted of subunits of lower hierarchical order. Fine aggregates comprised mainly microaggregates, whereas coarse aggregates were dominated by macroaggregates.

4.2. Mineralization rates of bulk soil versus aggregate size classes: a question of SOM bioavailability?

The cumulative CO_2–C respiration per unit mass SOC was comparable among the coarse aggregates, recombined bulk soil, and bulk soil (Fig. 4b). Its calculation from cumulative CO_2 emissions per unit mass soil depended on the unit mass SOC of each aggregate size class (Fig. 4a). This differentiation between

mineralization rates based on unit mass soil (Fernandez et al., 2010; Oorts et al., 2006) and unit mass SOC (Weintraub and Schimel, 2003) is important, but the two results are rarely presented at the same time (Bimüller et al., 2014). While the calculation based on unit mass soil predominantly considers the physical characteristics such as surface effects (Fig. 4a), the calculation based on SOC contents reflects the SOC pool and its bioavailable proportion (Fig. 4b).

Fine aggregates showed the highest respiration rates per unit mass soil (Fig. 4a) because the aggregate surface area increases as the size of the subunits decreases. These findings are in line with Drury et al. (2004). In general, microbes and enzymes have greater surface access to organic matter in smaller aggregates; in coarser aggregates, this matter is sequestered (Curtin et al., 2014). Such occlusion controls decomposition by restricting the oxygen movement to sites of microbiological activity (Baldock and Skjemstad, 2000). This property of a greater surface access in fine aggregates is reflected in the higher microbial quotients (Table 4).

The lower specific respiration rate per unit mass SOC in fine aggregates (Fig. 4b) was linked to the high SOC content (Table 1). SOC in coarse and fine aggregates probably differed in its chemical composition. According to Gupta and Germida (1988) and von Lützow et al. (2006), microaggregates have high stabilization capacity, which is enhanced by highly processed SOC and reduced oxygen diffusion (which restricts the aerobic decomposition). The organic matter in coarse aggregates was more labile and readily mineralizable (Fig. 4b) as shown by Elliott (1986) and Gupta and Germida (1988). Also the recent study of Tian et al. (2015) demonstrated a higher cumulative SOC-derived CO_2 production from macroaggregates >250 μm compared to microaggregates. The authors ascribed this to a higher proportion of more decomposable and less protected SOC within macroaggregates and emphasized that soil aggregate size class has clear effects on carbon mineralization. We conclude that SOC in fine aggregates with a higher surface area in comparison to coarse aggregates is less bioavailable to microorganisms.

Coarse aggregates contributed most to the total carbon mineralization because they were abundant in bulk soil. Recombined bulk soil equivalently respired to bulk soil (Fig. 4b) and mineralized carbon with similar efficiency to bulk soil (Table 4), proving that the aggregates were minimally disturbed during separation.

SOM bioavailability in fine aggregates, coarse aggregates, and bulk soil declined throughout the experiment, as shown by the decreasing MBC and MBN values (Table 2). This is consistent with SEOC being part of the bio-reactive labile carbon fraction. SEOC decreased during the experiment (Table 3) because this pool provided a readily available energy source for microorganisms (Akinsete and Nortcliff, 2014). However, the decline was low, indicating that aggregates conserved a supply of SEOC. In general, MBC and MBN values were lower in fine aggregates than in coarse aggregates (which were dominated by macroaggregates). Higher MBC and MBN contents in macroaggregates were also reported by Gupta and Germida (1988) and Miller and Dick (1995). However, unlike the rapidly declining SEOC values reported by Mueller et al. (2012), our intact aggregates functioned as a sustainable storage conserving microbial biomass. Microbial biomass, especially fungal biomass, plays an important role in the formation of macroaggregates associated with plant roots and root hairs (Oades, 1993) and delivers the labile organic matter that is easily respired (Gupta and Germida, 1988). In this way, microbial biomass increases the carbon mineralization rates in coarse aggregates (Fig. 4b). Supporting our findings, Jiang et al. (2011) identified the most biologically active microorganisms in aggregates of 1.0–2.0 mm diameter. MBC decreased faster in fine aggregates than in coarse aggregates and bulk soil, indicating a more rapid decline in bioavailability. The same trend was observed in MBN. The metabolic quotients declined throughout the experiment in all size classes (Table 4), indicating more efficient usage of the available organic matter after 224 days (Breland and Eltun, 1999). Between 14 and 224 days, the metabolic quotients of coarse and fine aggregates decreased by 45% and 58%, respectively. Consistent with Miller and Dick (1995), our coarse aggregates exhibited a lower metabolic quotient than fine aggregates (Table 4). MBC per unit mass SOC was also high in coarse aggregates (Table 2), indicating higher metabolic efficiency and more incorporation of SOC in these aggregates. Noting that coarse aggregates are dominated by macroaggregates, these results indicate a different bioavailability of SOM in macro- and microaggregates, as also found by Miller and Dick (1995).

In summary, a gentle aggregate separation into different size classes neither changed nor destroyed the microbial functionality of the aggregates in the different size classes, but provided a useful tool for assessing their role in microbial mineralization within bulk soil. We therefore conclude that the mineralization behavior in the aggregate size classes differed because of specific proportions of bioavailable SOM. The coarse aggregates mineralized more carbon per unit soil organic carbon than the fine aggregates. For nitrogen mineralization, it was vice versa.

4.3. Nitrogen mineralization is impaired by carbon limitation in laboratory incubation

The declining MBN was accompanied by an increase in SEON (Tables 2 and 3), but was not further mineralized. The N_{min} values were generally higher in fine than in coarse aggregates (Fig. 5) because the surface area increased with decreasing aggregate size. The mineralization rates per unit mass soil (Fig. 5a) and unit N_{tot} were quite similar, as the N_{tot} concentrations were more consistent than the SOC values among the aggregate classes (Table 1). In general, the N_{min} was similar in the recombined and measured bulk soil, again confirming that the soil structural units survived the aggregate separation and remained functionally intact. The mineralized nitrogen concentrations did not significantly change over time; the sharp decline in NH_4^+ concentration during the first two weeks suggests a nitrification to NO_3^-. In contrast to Oorts et al. (2006) and Weintraub and Schimel (2003) we observed no increase in cumulative nitrogen mineralization throughout the incubation time. All size classes were eventually limited by SOM bioavailability because the turnover of natural organic matter in the neutral topsoil of grassland (Oades, 1988) was prevented under our laboratory conditions.

In the regression of nitrogen mineralization against CO_2–C respiration, we observed negative gradients for all size classes, indicating that nitrogen mineralization did not proceed with carbon mineralization (Fig. 6). We attribute this result to the declining carbon bioavailability and lack of fresh SOM input. Once the bioavailability of organic carbon has fallen below the maintenance requirement of the microbial community, the living biomass declines (Anderson and Domsch, 1993).

In general, our study yielded lower carbon and nitrogen mineralization levels per unit mass soil and unit mass SOC than comparable incubation studies in literature, such as Curtin et al. (2014), whose investigation lasted for ≥100 days. Other studies might have provided mechanical energy during the aggregate fractionation (Curtin et al., 2014), providing more easily mineralizable material and breaking down the soil structure as the aggregates were crushed (Chevallier et al., 2011). This was avoided by our gentle aggregate preparation prior to incubation.

In summary, nitrogen mineralization was impaired by carbon limitation as the incubation experiment proceeded.

4.4. Soil organic matter stabilization mechanisms in aggregates

Coarse aggregates respired more CO_2–C per unit mass SOC than the other size classes, probably because they were less stable and their organic material composition differed from fine aggregates. Less than 10% of the SOC was recovered in the light fraction of the studied soil (Kreyling et al., 2013), equating the labile pool that is easily turned over. According to previous research, if SOC is the dominant binding agent for micro-within-macroaggregates (Six and Paustian, 2014), the SOC concentration should be greater in aggregates of higher hierarchical order (Oades and Waters, 1991; Rabbi et al., 2015). The specific higher respiration in coarse aggregates (Fig. 4b) indicates greater SOM bioavailability, most likely because the smaller macro- and microaggregates are stabilized at the macroaggregate level by labile SOM and exocellular mucilage of microorganisms (Miller and Dick, 1995; Tisdall and Oades, 1982). This labile SOM, which can be rapidly respired, adheres smaller aggregates and stabilizes coarse aggregates (Cambardella and Elliott, 1994). However, due to the rapid turnover, our grassland soil is characterized by low concentration of particulate organic matter (Oades, 1984, 1988). Moreover, the artificial laboratory incubation excludes any fresh organic input that would be rapidly mineralized under natural grassland conditions.

We can attribute the high degree of SOM stabilization in fine aggregates to the tighter stabilization mechanism in these structures, which are mainly built of microaggregates. This mechanism includes cation bridging (Baldock and Skjemstad, 2000; La Mer, 1964; Labille et al., 2003; Lafuma et al., 1991; Oades, 1984). In fact, the multiplication of such bridges leads to microaggregate formation (Adachi, 1995; Labille et al., 2003). Within such tightly fixed stable structures, SOC is unavailable to microorganisms and cannot be respired, as demonstrated by the higher SOC values (Table 1) and lower CO_2–C respiration per unit mass SOC (Fig. 4b) in fine aggregates than in coarse aggregates. Since calcium controls organo-mineral complexation, it generally exerts a direct stabilizing effect at the microaggregate level, but can also incidentally stimulate macroaggregation by optimal conditions for microbial activity due to an ideal milieu (Six et al., 2004).

We conclude that calcium-clay bridges may stabilize SOM at the microaggregate level in our dolomitic soil, whereas labile SOM (including mucilage) adheres these microaggregates into macroaggregates of higher hierarchical orders.

5. Conclusions

The incubation of intact aggregate classes differing in size revealed distinct carbon and nitrogen bioavailabilites due to a specific aggregate architecture. Future studies on carbon and nitrogen mineralization in natural coarse and fine aggregates should consider (1) the different aggregate architectures of the size classes and (2) the increased surface area of smaller aggregate diameters. These physical characteristics are taken into account by referring mineralization on unit soil mass. Despite the higher surface area in fine aggregates, a smaller proportion of SOM was bioavailable in fine aggregates than in coarse ones. Therefore, future studies should also consider (3) the proportion of bioavailable SOM bound into aggregates, which was effectively depleted in the fine aggregates of our soil. The bioavailable proportion of the SOM pool can be estimated by referring carbon and nitrogen mineralization on SOC and N_{tot} content, respectively. Carbon mineralization normalized to the SOC content was smaller in the fine aggregates (<2 mm) than that in the coarse aggregates (2–6.3 mm), indicating that SOC stabilization was stronger in fine aggregates. Accordingly, MBC and MBN contents decreased particularly rapidly in fine aggregates throughout the experiment. This indicated a declining and lower bioavailability of SOM in fine aggregates and an enhanced stabilization through cation bridging of the dolomitic soil material at the microaggregate level. Bioavailability of SOM was higher in the coarse aggregates, which comprised smaller macro- and microaggregates adhered by labile microbial mucilage.

Acknowledgements

We thank Sigrid Hiesch for laboratory assistance. Two anonymous reviewers and the editor are gratefully acknowledged for their helpful comments. This study was supported by a grant from the Bavarian State Ministry of Education, Science and the Arts.

References

Adachi, Y., 1995. Dynamic aspects of coagulation and flocculation. Adv. Colloid Interface Sci. 56, 1–31.
Akinsete, S.J., Nortcliff, S., 2014. Storage of total and labile soil carbon fractions under different land-use types: a laboratory incubation study. Soil Carbon. In: Hartemink, A.E., McSweeney, K. (Eds.), Progress in Soil Science. Springer International Publishing Switzerland.
Alef, K., Nannipieri, P., 1995. Methods in Applied Soil Microbiology and Biochemistry. Academic Press, London [u.a.].
Álvarez, S., Soriano, M.A., Landa, B.B., Gómez, J.A., 2007. Soil properties in organic olive groves compared with that in natural areas in a mountainous landscape in southern Spain. Soil Use Manage. 23, 404–416.
Amelung, W., Zech, W., 1999. Minimisation of organic matter disruption during particle-size fractionation of grassland epipedons. Geoderma 92, 73–85.
Anderson, T.H., Domsch, K.H., 1993. The metabolic quotient for CO_2 (qCO_2) as a specific activity parameter to assess the effects of environmental conditions, such as pF, on the microbial biomass of forest soils. Soil Biol. Biochem. 25, 393–395.
Baker, J.M., Ochsner, T.E., Venterea, R.T., Griffis, T.J., 2007. Tillage and soil carbon sequestration—What do we really know? Agric. Ecosyst. Environ. 118, 1–5.
Baldock, J.A., Oades, J.M., Nelson, P.N., Skene, T.M., Golchin, A., Clarke, P., 1997. Assessing the extent of decomposition of natural organic materials using solid-state C-13 NMR spectroscopy. Aust. J. Soil Res. 35, 1061–1083.
Baldock, J.A., Skjemstad, J.O., 2000. Role of the soil matrix and minerals in protecting natural organic materials against biological attack. Org. Geochem. 31, 697–710.
Beare, M.H., Cabrera, M.L., Hendrix, P.F., Coleman, D.C., 1994. Aggregate-protected and unprotected organic-matter pools in conventional-tillage and no-tillage soils. Soil Sci. Soc. Am. J. 58, 787–795.
Bertrand, I., Delfosse, O., Mary, B., 2007. Carbon and nitrogen mineralization in acidic, limed and calcareous agricultural soils: apparent and actual effects. Soil Biol. Biochem. 39, 276–288.
Bimüller, C., Mueller, C.W., von Lutzow, M., Kreyling, O., Kölbl, A., Haug, S., Schloter, M., Kögel-Knabner, I., 2014. Decoupled carbon and nitrogen mineralization in soil particle size fractions of a forest topsoil. Soil Biol. Biochem. 78, 263–273.
Bockenhoff, K., Gall, S., Fischer, W.R., 1997. Surface charge of clay-humus fractions from Chernozems as a function of pH and Ca-concentration. Zeitschrift Für Pflanzenernährung und Bodenkunde 160, 341–346.
Breland, T.A., Eltun, R., 1999. Soil microbial biomass and mineralization of carbon and nitrogen in ecological, integrated and conventional forage and arable cropping systems. Biol. Fertil. Soils 30, 193–201.
Cambardella, C.A., Elliott, E.T., 1994. Carbon and nitrogen dynamics of soil organic matter fractions from cultivated grassland soils. Soil Sci. Soc. Am. J. 58, 123–130.
Chevallier, T., Blanchart, E., Toucet, J., Bernoux, M., 2011. Methods to estimate aggregate protected soil organic carbon, 2: does the grinding of the plant residues affect the estimations of the aggregate protected soil organic carbon? Commun. Soil Sci. Plant Anal. 42, 1537–1543.
Collins, H.P., Elliott, E.T., Paustian, K., Bundy, L.C., Dick, W.A., Huggins, D.R., Smucker, A.J.M., Paul, E.A., 2000. Soil carbon pools and fluxes in long-term corn belt agroecosystems. Soil Biol. Biochem. 32, 157–168.
Curtin, D., Beare, M.H., Scott, C.L., Hernandez-Ramirez, G., Meenken, E.D., 2014. Mineralization of soil carbon and nitrogen following physical disturbance: a laboratory assessment. Soil Sci. Soc. Am. J. 78, 925–935.
Drury, C.F., Yang, X.M., Reynolds, W.D., Tan, C.S., 2004. Influence of crop rotation and aggregate size on carbon dioxide production and denitrification. Soil Till. Res. 79, 87–100.
Elliott, E.T., 1986. Aggregate structure and carbon, nitrogen, and phosphorus in native and cultivated soils. Soil Sci. Soc. Am. J. 50, 627–633.
Fernandez, R., Quiroga, A., Zorati, C., Noellemeyer, E., 2010. Carbon contents and respiration rates of aggregate size fractions under no-till and conventional tillage. Soil Till. Res. 109, 103–109.
Franzluebbers, A.J., Haney, R.L., Hons, F.M., Zuberer, D.A., 1996. Determination of microbial biomass and nitrogen mineralization following rewetting of dried soil. Soil Sci. Soc. Am. J. 60, 1133–1139.
Gupta, V.V.S.R., Germida, J.J., 1988. Distribution of microbial biomass and its activity in different soil aggregate size classes as affected by cultivation. Soil Biol. Biochem. 20, 777–786.

Gupta, V.V.S.R., Germida, J.J., 2015. Soil aggregation: Influence on microbial biomass and implications for biological processes. Soil Biol. Biochem. 80, A3–A9.
IUSS Working Group WRB, 2014. World Reference Base for Soil Resources 2014. International soil classification system for naming soils and creating legends for soil maps. World Soil Resources Reports No. 106. FAO, Rome.
Jiang, X., Wright, A.L., Wang, J., Li, Z., 2011. Long-term tillage effects on the distribution patterns of microbial biomass and activities within soil aggregates. Catena 87, 276–280.
Kölbl, A., Leifeld, J., Kögel-Knabner, I., 2005. A comparison of two methods for the isolation of free and occluded particulate organic matter. J. Plant Nutr. Soil Sci. Zeitschrift Für Pflanzenernährung und Bodenkunde 168, 660–667.
Kreyling, O., Kölbl, A., Spielvogel, S., Rennert, T., Kaiser, K., Kögel-Knabner, I., 2013. Density fractionation of organic matter in dolomite-derived soils. J. Plant Nutr. Soil Sci. Zeitschrift Für Pflanzenernährung und Bodenkunde 176, 509–519.
La Mer, V.K., 1964. Coagulation symposium introduction. J. Colloid Sci. 19, 291–293.
Labille, J., Thomas, F., Bihannic, I., Santella, C., 2003. Destabilization of montmorillonite suspensions by Ca2+ and succinoglycan. Clay Miner. 38, 173–185.
Lafuma, F., Wong, K., Cabane, B., 1991. Bridging of colloidal particles through adsorbed polymers. J. Colloid Interface Sci. 143, 9–21.
Mikha, M.M., Rice, C.W., 2004. Tillage and manure effects on soil and aggregate-associated carbon and nitrogen. Soil Sci. Soc. Am. J. 68, 809–816.
Miller, M., Dick, R.P., 1995. Dynamics of soil C and microbial biomass in whole soil and aggregates in 2 cropping systems. Appl. Soil Ecol. 2, 253–261.
Mueller, C.W., Schlund, S., Prietzel, J., Kögel-Knabner, I., Gutsch, M., 2012. Soil aggregate destruction by ultrasonication increases soil organic matter mineralization and mobility. Soil Sci. Soc. Am. J. 76, 1634–1643.
Nyamadzawo, G., Nyamangara, J., Nyamugafata, P., Muzulu, A., 2009. Soil microbial biomass and mineralization of aggregate protected carbon in fallow-maize systems under conventional and no-tillage in Central Zimbabwe. Soil Till. Res. 102, 151–157.
Oades, J.M., 1984. Soil organic matter and structural stability: mechanisms and implications for management. Plant Soil 76, 319–337.
Oades, J.M., 1988. The retention of organic matter in soils. Biogeochemistry 5, 35–70.
Oades, J.M., 1993. The role of biology in the formation, stabilization and degradation of soil structure. Geoderma 56, 377–400.
Oades, J.M., Waters, A.G., 1991. Aggregate hierarchy in soils. Aust. J. Soil Res. 29, 815–828.
Oorts, K., Nicolardot, B., Merckx, R., Richard, G., Boizard, H., 2006. C and N mineralization of undisrupted and disrupted soil from different structural zones of conventional tillage and no-tillage systems in northern France. Soil Biol. Biochem. 38, 2576–2586.
Petersen, S.O., Klug, M.J., 1994. Effects of sieving storage, and incubation-temperature on the phospholipid fatty-acid profile of a soil mircobial community. Appl. Environ. Microbiol. 60, 2421–2430.
Rabbi, S.M.F., Wilson, B.R., Lockwood, P.V., Daniel, H., Young, I.M., 2015. Aggregate hierarchy and carbon mineralization in two Oxisols of New South Wales, Australia. Soil Till. Res. 146, 193–203.
Rashad, M., Dultz, S., Guggenberger, G., 2010. Dissolved organic matter release and retention in an alkaline soil from the Nile River Delta in relation to surface charge and electrolyte type. Geoderma 158, 385–391.
Sainju, U.M., Caesar-TonThat, T., Jabro, J.D., 2009. Carbon and nitrogen fractions in dryland soil aggregates affected by long-term tillage and cropping sequence. Soil Sci. Soc. Am. J. 73, 1488–1495.
Schlichting, E., Blume, H.P., Stahr, K., 1995. Bodenkundliches Praktikum, 2nd ed. Blackwell Wissenschafts-Verlag, Berlin Wien.
Six, J., Elliott, E.T., Paustian, K., 2000. Soil macroaggregate turnover and microaggregate formation: a mechanism for C sequestration under no-tillage agriculture. Soil Biol. Biochem. 32, 2099–2103.
Six, J., Bossuyt, H., Degryze, S., Denef, K., 2004. A history of research on the link between (micro) aggregates, soil biota, and soil organic matter dynamics. Soil Till. Res. 79, 7–31.
Six, J., Paustian, K., 2014. Aggregate-associated soil organic matter as an ecosystem property and a measurement tool. Soil Biol. Biochem. 68, A4–A9.
Stemmer, M., Von Lützow, M., Kandeler, E., Pichlmayer, F., Gerzabek, M.H., 1999. The effect of maize straw placement on mineralization of C and N in soil particle size fractions. Eur. J. Soil Sci. 50, 73–85.
Tian, J., Pausch, J., Yu, G., Blagodatskaya, E., Gao, Y., Kuzyakov, Y., 2015. Aggregate size and their disruption affect 14C-labeled glucose mineralization and priming effect. Appl. Soil Ecol. 90, 1–10.
Tisdall, J.M., Oades, J.M., 1982. Organic matter and water-stable aggregates in soils. J. Soil Sci. 33, 141–163.
Unteregelsbacher, S., Gasche, R., Lipp, L., Sun, W., Kreyling, O., Geitlinger, H., Kogel-Knabner, I., Papen, H., Kiese, R., Schmid, H.P., Dannenmann, M., 2013. Increased methane uptake but unchanged nitrous oxide flux in montane grasslands under simulated climate change conditions. Eur. J. Soil Sci. 64, 586–596.
Vance, E.D., Brookes, P.C., Jenkinson, D.S., 1987. An extraction method for measuring soil microbial biomass C. Soil Biol. Biochem. 19, 703–707.
von Lützow, M., Kögel-Knabner, I., Ekschmitt, K., Matzner, E., Guggenberger, G., Marschner, B., Flessa, H., 2006. Stabilization of organic matter in temperate soils: mechanisms and their relevance under different soil conditions—a review. Eur. J. Soil Sci. 57, 426–445.
Weintraub, M.N., Schimel, J.P., 2003. Interactions between carbon and nitrogen mineralization and soil organic matter chemistry in arctic tundra soils. Ecosystems 6, 129–143.
Zhang, S.X., Li, Q., Zhang, X.P., Wei, K., Chen, L.J., Liang, W.J., 2012. Effects of conservation tillage on soil aggregation and aggregate binding agents in black soil of Northeast China. Soil Till. Res. 124, 196–202.